Cancer Therapy: Preclinical

Clinical Cancer Research

Counteracting Autophagy Overcomes Resistance to Everolimus in Mantle Cell Lymphoma

Laia Rosich, Sílvia Xargay-Torrent, Mónica López-Guerra, Elías Campo, Dolors Colomer, and Gaël Roué

Abstract

Purpose: Mantle cell lymphoma (MCL) is an aggressive B-lymphoid neoplasm with poor response to conventional chemotherapy and short survival. The phosphatidylinositol 3-kinase/Akt/mTOR survival pathway is constitutively activated in MCL cells, thereby making the mTOR inhibition an attractive therapeutic strategy. The first clinical studies of everolimus (RAD001), an mTOR inhibitor, in relapsed MCL patients have reported a significant response. Our aim was to analyze the mechanism related to everolimus resistance/sensitivity in MCL cells.

Experimental Design: Sensitivity to everolimus was analyzed in MCL cell lines and primary MCL cells. Everolimus mechanism of action was determined by flow cytometry and Western blot. Particularly, autophagy was studied by LC3BI/II expression, autophagolysosomes detection by flow cytometry and fluorescence microscopy, and siRNA-mediated gene silencing.

Results: Everolimus exerted antitumoral effect on MCL cells while sparing normal cells. In MCL cell lines, this phenomenon was associated to G_1 cell-cycle arrest, dephosphorylation of the mTOR downstream targets, 4E-BP1 and S6RP, and rephosphorylation of Akt. A synergistic cytotoxic effect was observed between everolimus and an Akt inhibitor, which overcame the compensatory reactivation within the mTOR signaling pathway. Interestingly, MCL cells with low response to this combination showed high levels of autophagy. Accordingly, selective triple knockdown of the autophagy genes *ATG7*, *ATG5* and *ATG3*, and pretreatment with the autophagy inhibitor hydroxychloroquine, efficiently overcame the resistance to Akt/mTOR inhibitors, leading to the activation of the mitochondrial apoptotic pathway.

Conclusions: These results suggest that autophagy induction protects MCL cells from Akt/mTOR targeting and counteracting autophagy may represent an attractive strategy for sensitizing MCL cells to everolimus-based therapy. *Clin Cancer Res; 18(19); 5278–89. ©2012 AACR.*

Introduction

Mantle cell lymphoma (MCL) is an aggressive lymphoid neoplasm that accounts for 5% to 10% of all B-cell non-Hodgkin's lymphomas. It is genetically characterized by the chromosomal translocation t(11;14)(q13;q32) resulting in overexpression of cyclin D1. Moreover, high levels of chromosomal instability related to the disruption of the DNA damage response pathway and activation of cell survival mechanisms may confer an aggressive clinical course to the disease (1). Standard chemotherapy approaches are frequently used, but long-term remissions are rare. After failure of first- or second-line treatments, various single agents are used despite limited response rates (2). Thus, there is still a strong unmet medical need for new treatment options in MCL.

The constitutive activation of the phosphatidylinositol 3-kinase (PI3K) and the serine/threonine kinases Akt and mTOR are known to confer drug resistance to many types of cancer, including MCL (2). Thus, this pathway has emerged as a promising therapeutic target. mTOR is an evolutionarily conserved kinase that integrates signals from growth factors, nutrients, and stresses to regulate multiple processes, including mRNA translation, cell-cycle progression, autophagy, and cell survival. mTOR resides in 2 distinct multiprotein complexes referred to as mTOR complex 1 (mTORC1) and mTOR complex 2 (mTORC2). By phosphorylating S6 kinase 1 and the eIF4E-binding protein 1 (4E-BP1), mTORC1 controls the translation of key regulatory proteins involved in cell proliferation (3). mTORC2 modulates cell survival in response to growth factors by phosphorylation of its downstream effectors Akt and serum/glucocorticoid regulated kinase 1 (4). In addition to directly activate Akt as part of mTORC2, mTOR, as part of

Authors' Affiliation: Hematopathology Unit, Hospital Clínic, Institut d'Investigacions Biomèdiques August Pi i Sunyer (IDIBAPS), Universitat de Barcelona, Barcelona, Spain

Note: Supplementary data for this article are available at Clinical Cancer Research Online (http://clincancerres.aacrjournals.org/).

D. Colomer and G. Roué share the senior authorship of this article.

Corresponding Author: Gaël Roué, IDIBAPS, Hemato-oncology Department, Rosselló, 153, 08036 Barcelona, Spain. Phone: 34-932-275-400, ext 4525; Fax: 34-933-129-407; E-mail: groue@clinic.ub.es

doi: 10.1158/1078-0432.CCR-12-0351

Translational Relevance

Mantle cell lymphoma (MCL) is an aggressive neoplasm that lacks effective therapy. The mTOR kinase inhibitor everolimus (RAD001) has shown activity in preclinical and clinical models of MCL, although its mechanism of action has not been fully elucidated. Here, we find that everolimus activity in MCL cell lines and primary cultures is closely linked to Akt phosphorylation status, and that the prevention of Akt rephosphorylation upon everolimus treatment by means of a selective Akt inhibitor greatly enhances everolimus activity in MCL cells. Furthermore, our data reported here show that an accumulation of autophagic vacuoles may limit the efficacy of dual Akt/mTOR targeting in resistant cells, and that secondary inhibition of autophagosome formation completes the therapeutic potential of this strategy. We thus provide the proof of principle and rationale for further clinical evaluation of Akt/mTOR and autophagy triple targeting to improve patient outcome in MCL.

mTORC1, also negatively regulates Akt by suppressing growth factor–driven pathways (5).

The macrocyclic lactone antibiotic rapamycin (sirolimus), an allosteric mTORC1 inhibitor isolated from *Streptomyces hygroscopicus*, was found to possess immunosuppressive and antiproliferative properties. More recently, 3 rapamycin derivatives (termed rapalogs)—temsirolimus (CCI-779), ridaforolimus (AP23573, MK-8669), and everolimus (RAD001)—with improved properties were developed (6). Temsirolimus was approved by the European Medicines Agency for the treatment of relapsed and refractory MCL, while ridaforolimus and everolimus have been studied in various clinical trials (7). These rapalogs have reported a moderate success as monotherapy with mild toxic effects, with an observed half-life of about 30 hours (8, 9). A recent phase II study of everolimus reported a 32% overall response rate in MCL patients (10), which is similar to that found in other trials using temsirolimus (11–13). However, the effectiveness of these agents as single agent therapies is stifled in part by strong mTORC1-dependent negative feedback loops that become inactive on mTORC1 inhibition, paradoxically leading to survival promoting events such as the activation of Akt (5, 14). Thus, these compounds may represent good candidates in combination with chemotherapy and targeted agents capable of counteracting these mechanisms of resistance (15).

In this context, our purpose was to describe the molecular bases of MCL cell response to everolimus, with the aim to validate new possible combination strategies. Herein, we show that everolimus induces the rephosphorylation of Akt, mediated by a feedback loop within the PI3K/Akt/mTOR axis that can be blocked by the Akt inhibitor VIII isozyme-selective Akti-1/2. We also show the protective effect of autophagy to actively counteract everolimus and Akti-1/2 activity in MCL cell lines and primary samples. Thus, we propose the triple targeting of mTOR, Akt, and autophagy as a requisite for effective antitumoral therapy in MCL.

Materials and Methods

Cell lines

The MCL cell lines REC-1, JEKO-1, GRANTA-519, UPN-1, HBL-2, JVM-2, MAVER-1, and Z-138 (Table 1) used in this study were cultured in RPMI 1640 or Dulbecco's Modified Eagle's Medium, supplemented with 10% to 20% heat-inactivated FBS, 2 mmol/L glutamine and 50 μg/mL penicillin-streptomycin (Life Technologies). All cultures were routinely tested for *Mycoplasma* contamination by PCR and the identity of all cell lines was verified by using AmpFISTR identifier kit (Life Technologies).

Isolation and culture of primary cells

Cells from 11 patients diagnosed with MCL according to the World Health Organization classification criteria (16), who had not received treatment for the 3 previous months, were used. The clinical characteristics of these patients are listed in Table 1. Informed consent was obtained from each patient in accordance with the guidelines of the Ethical Committee of the Hospital Clinic in Barcelona, Spain, and the Declaration of Helsinki. For all samples, cyclin D1 overexpression was determined by immunohistochemistry or real-time PCR. *P53* mutational status was assessed by FISH and direct sequencing. Mononuclear cells from peripheral blood samples (PBMC) were isolated by Ficoll/hypaque sedimentation (GE Healthcare), and conserved within the Hematopathology Biobank of our institution (CDB Biobank/IDIBAPS-Hospital Clínic Biobank). Cells were either used directly or cryopreserved in liquid nitrogen in the presence of 10% dimethyl sulfoxide, 60% FBS, and 30% RPMI 1640. Freezing/thawing manipulations did not influence cell response (17).

Treatments and assessment of apoptosis by flow cytometry

Cells received as indicated a single treatment of everolimus (kindly provided by Novartis), Akt inhibitor VIII isozyme-selective Akti-1/2 (Calbiochem), hydroxychloroquine sulfate (Sigma), bafilomycin A1 (Sigma), and tamoxifen (Enzo Life Sciences). Cell viability was quantified by staining of external exposure of phosphatidylserine (PS) residues with Annexin V-fluorescein isothiocyanate (FITC) and propidium iodide (PI; Bender Medsystems). For the analysis of apoptosis in $CD3^+$ and $CD19^+$ subpopulations, PBMCs were labeled simultaneously with anti-CD3-FITC, anti-CD19-Phycoerythrin (PE; Becton Dickinson) antibodies, and Annexin V-allophycocyanin (APC; Bender Medsystems). Changes in mitochondrial transmembrane potential ($\Delta\psi m$) and reactive oxygen species (ROS) production were evaluated by staining cells with 20 nmol/L 3,3′-diexyloxacarbocyanine iodide ($DiOC_6[3]$; Life Technologies) and 2 μmol/L dihydroethidine (DHE; Life Technologies), respectively. For the quantification of caspase-3/

Table 1. Characteristics of MCL cell lines and primary samples

MCL cell line	% cytostatic effect 24 h, 5 μmol/L	% cytostatic effect 72 h, 5 μmol/L	GI_{50} 72 h, nmol/L	% cytotoxicity 72 h, 5 μmol/L	Genetic alterations		
					P53[a]	ATM	P16
Z-138	16.82	16.88	NR	6.08	wt	del/[b]	del
MAVER-1	18.85	31.89	NR	5.12	del/mut	del/[b]	del
JVM-2	16.09	34.41	NR	4.71	wt	wt	wt
HBL-2	8	45.10	NR	1.23	del/mut	upd	del
UPN-1	22.28	62.73	125.7	4.25	del/mut	wt	del/[b]
GRANTA-519	19.94	63.30	62.88	10.54	del/wt	del/mut	del
JEKO-1	21.16	68.52	25.5	8.61	del/mut	ampl/[b]	del/[b]
REC-1	23.38	69.38	4.35	10.69	wt	wt/[b]	del

Patient no.	LD_{50} 48 h, μmol/L	% cytotoxicity 48 h, 5 μmol/L	Disease status	Morphologic variant	% of tumor cells[c]	P53[a] status
1	NR	8.64	Diagnosis	Classical	77	wt
2	NR	10.4	Diagnosis	Blastoid	94	wt
3	NR	20.2	Diagnosis	Classical	97	wt
4	NR	25.4	Diagnosis	Classical	85	wt
5	NR	28.9	Diagnosis	Classical	79	del/wt
6	NR	31.2	Diagnosis	Classical	96	del/wt
7	3.89	38.7	Diagnosis	Classical	89	wt
8	3.81	63.2	Diagnosis	Blastoid	80	wt
9	3.62	67.6	Diagnosis	Classical	83	wt
10	3.84	69.6	Diagnosis	Classical	86	wt
11	4.03	73.5	Diagnosis	Classical	91	del/mut

Abbreviations: NR, not reached; wt, wild type; del, deletion; mut, mutation; ampl, amplification; upd, uniparental disomy.

[a]*P53* mutational status assessed by FISH and direct sequencing.

[b]Mutations not analyzed.

[c]CD19+ tumor cells quantified by flow cytometry.

7 activity, cells were labeled with 2 μmol/L CellEvent caspase-3/7 green detection reagent (Life Technologies) for 30 minutes at 37°C. A total of 10,000 stained cells per sample were acquired and analyzed in a FACScan or FACSCalibur flow cytometer by using Cellquest and Paint-A-Gate softwares (Becton Dickinson). Lethal dose 50 (LD_{50}) was defined as the concentration of drug required to reduce cell viability by 50%. In drug combination studies, combination index (CI) values were calculated according to the Chou–Talalay method by means of the Calcusyn software version 2.0 (Biosoft), where CI < 1 indicated synergistic effect between 2 drugs.

Cell proliferation assay

MCL cell lines (5×10^4) were incubated for 72 hours with everolimus. MTT [3-(4,5-dimethylthiazolyl-2)-2,5-diphenyltetrazolium bromide] reagent (Sigma) was added for 2 to 5 additional hours before spectrophotometric measurement. Each measurement was made in triplicate, and the mean value was calculated. For each cell line, values were represented using untreated control cells as a reference. The growth inhibitory activity 50 (GI_{50}) was calculated as the dose that produced 50% growth inhibition.

Cell-cycle analysis

Cells were incubated for 72 hours with everolimus, washed in PBS and fixed with 70% ethanol. After incubation with PI for 30 minutes at 37°C, cell-cycle fractions were determined by flow cytometry (FACScan). The analysis was conducted by applying the ModFit LT software (Verity Software House).

Western blot analysis

Whole-cell protein extracts were obtained by lysing cells in Triton buffer (20 mmol/L Tris-HCL pH 7.6, 150 mmol/L NaCl, 1 mmol/L EDTA, and 1% Triton X-100) supplemented with protease and phosphatase inhibitors (10 μg/mL leupeptin, 10 μg/mL aprotinin, 1 mmol/L phenylmethanesulfonyl fluoride, 5 mmol/L NaF, and 2 mmol/L Na_3VO_4). Solubilized proteins were quantified by Bradford protein assay and 50 μg of cell lysates were loaded onto 12% to 15% SDS-PAGE and transferred to an Immobilon-P membrane (Millipore). Membranes were blocked in TBS-Tween 20 containing 5% phosphoBlocker Blocking Reagent (Cell Biolabs) and probed with antibodies against: phospho-mTOR (Ser2448), phospho-Akt (Ser473), phospho-S6 ribosomal protein (S6RP; Ser235/236), phospho-4E-BP1

(Thr37/46), mTOR, Akt, S6RP, 4E-BP1, cleaved caspase-3 (Asp175, clone 5A1E), LC3B, ATG5 (D1G9) and ATG3 (Cell Signaling Technology), PARP (Roche), and ATG7 (clone EP1759Y; Abcam). Membranes were then incubated with horseradish peroxidase-labeled anti-mouse or anti-rabbit (Sigma and Cell Signaling Technologies) secondary antibodies. Chemiluminiscence detection was done by using ECL system (Pierce) in a mini-LAS4000 Fujifilm device, and relative protein quantification of LC3B was conducted with Image Gauge software (Fujifilm). Equal protein loading was confirmed by analyzing α-tubulin expression (Sigma).

Autophagolysosome detection

Samples containing 5×10^5 to 1×10^6 cells were stained for autophagolysosome contents with Cyto-ID Green Detection Reagent (Enzo Life Sciences) as described (18) for 30 minutes at 37°C, and the intensity of the green fluorescence was measured by flow cytometry (FACScan). Results were represented as histogram overlays. Hoechst 33342 Nuclear Stain was added to the Cyto-ID Green Detection Reagent stained cell suspension and applied to a glass microscope slide, covered with a cover slip and visualized on a Olympus BX41 microscopy (×40 objective) with the use of Cell ℛID Imagine Software (Olympus).

RNA interference assay

Z-138 cells (5×10^6) were cultured for 24 hours without antibiotics and washed with FBS-free RPMI medium. Cells were then electroporated with a Nucleofector II device (Lonza) in 100 μL of Ingenio Electroporation Solution (Mirus) containing 10 μmol/L of a mix of 6 different Silencer Select Predesigned siRNAs targeting *ATG7*, *ATG5*, and *ATG3*, and a nonsilencing negative control (Ambion). C-005 Nucleofector program was used. After transfection, cells were transferred to culture plates for 6 hours before experiments were set up.

Statistical analysis

Data are represented as mean ± SD or SEM of 3 independent experiments. Statistical analysis was conducted with the use of GraphPad Prism 4.0 software (GraphPad Software). Two-way ANOVA was used to determine how response is affected by 2 factors. Results were considered statistically significant when P value < 0.05 (*, $P < 0.05$, **, $P < 0.01$, ***, $P < 0.001$).

Results

Everolimus exerts selective antitumoral effect in MCL cells

To explore the antitumoral effect of everolimus, a panel of 8 MCL cell lines and 11 MCL primary samples were exposed for 48 hours (primary cells) or 72 hours (cell lines) to increasing doses of the drug (0.05, 0.5, and 5 μmol/L). Apoptosis induction and drug cytostatic effect were determined simultaneously by flow cytometry and MTT proliferation assay, respectively. As shown on Fig. 1A, everolimus mainly induced a cytostatic effect in MCL cell lines in a dose-dependent manner with minor (< 11%) cytotoxic activity (Table 1). In the high-sensitive MCL cell lines (UPN-1, GRANTA-519, JEKO-1, and REC-1), most of this effect (>50% antiproliferative activity) was reached at the lowest dose tested (0.05 μmol/L), with a GI_{50} < 130 nmol/L. In contrast, the low-sensitive cell lines (Z-138, MAVER-1, JVM-2, and HBL-2) did not undergo a marked proliferation decrease after everolimus treatment at doses below 5 μmol/L. In these cell lines, the GI_{50} at 72 hours could not be reached (Table 1). Consistently, cell-cycle analysis of 3 representative cell lines revealed a blockade in G_0–G_1 phase in the sensitive cells REC-1 and GRANTA-519, whereas the low sensitive Z-138 cells showed only a slight increase in the S phase cell fraction (Fig. 1B).

MCL primary cells showed a high sensitivity to the compound as a cytotoxic effect was detected in the majority of the samples as soon as 48 hours of treatment, contrasting with the low cell death rates observed in the cell lines, even after a 72-hour exposure to everolimus (Fig. 1C and Table 1). Five cases (MCL no. 7, 8, 9, 10, and 11) were sensitive to everolimus, with a mean LD_{50} of 3.84 ± 0.15 μmol/L, whereas 6 cases (MCL no. 1, 2, 3, 4, 5, and 6) showed a lower response to the drug (LD_{50} > 5 μmol/L; Table 1). This cytotoxic effect was shown to be selective as neither normal B ($CD19^+$) nor normal T lymphocytes ($CD3^+$) from healthy donors were notably affected by 5 μmol/L everolimus (Fig. 1C).

Of note, there was no association between MCL sensitivity to everolimus and common cytogenetic alterations such as deletions of *P53*, *ATM*, or *P16*, either in MCL cell lines or primary cells (Table 1).

Thus, these results show that everolimus induces apoptosis in the majority of MCL primary samples, at physiologically achievable doses, sparing normal B and T cells.

Everolimus modulates mTOR signaling pathway in MCL cells

To ensure that everolimus activity in MCL cell lines and primary MCL cells was linked to mTOR pathway inhibition, REC-1, GRANTA-519, Z-138 cells, and a representative MCL primary sample were treated with everolimus (doses ranging from 0.05 to 5 μmol/L) for up to 72 hours. Fig. 2A and B shows that short time incubation (24 hours) with everolimus in REC-1 and GRANTA-519 cells caused a dose-dependent decrease in the phosphorylation levels of Akt, mTOR, and its downstream targets, S6RP and 4E-BP1. About 4E-BP1, while the hyperphosphorylated isoforms decreased, the hypophosphorylated form accumulated after everolimus treatment. Interestingly, part of these effects was not sustained and after prolonged exposure to everolimus (48–72 hours), we observed a rephosphorylation of Akt and mTOR. In contrast, in the low-sensitive Z-138 cell line, everolimus only induced a transient downregulation of p-S6RP and p-4E-BP1 proteins, with no substantial changes in the levels of phospho-mTOR and a slight decrease in Akt phosphorylation at the higher dose and time of exposure (Fig. 2C). Importantly, everolimus efficiently inhibited

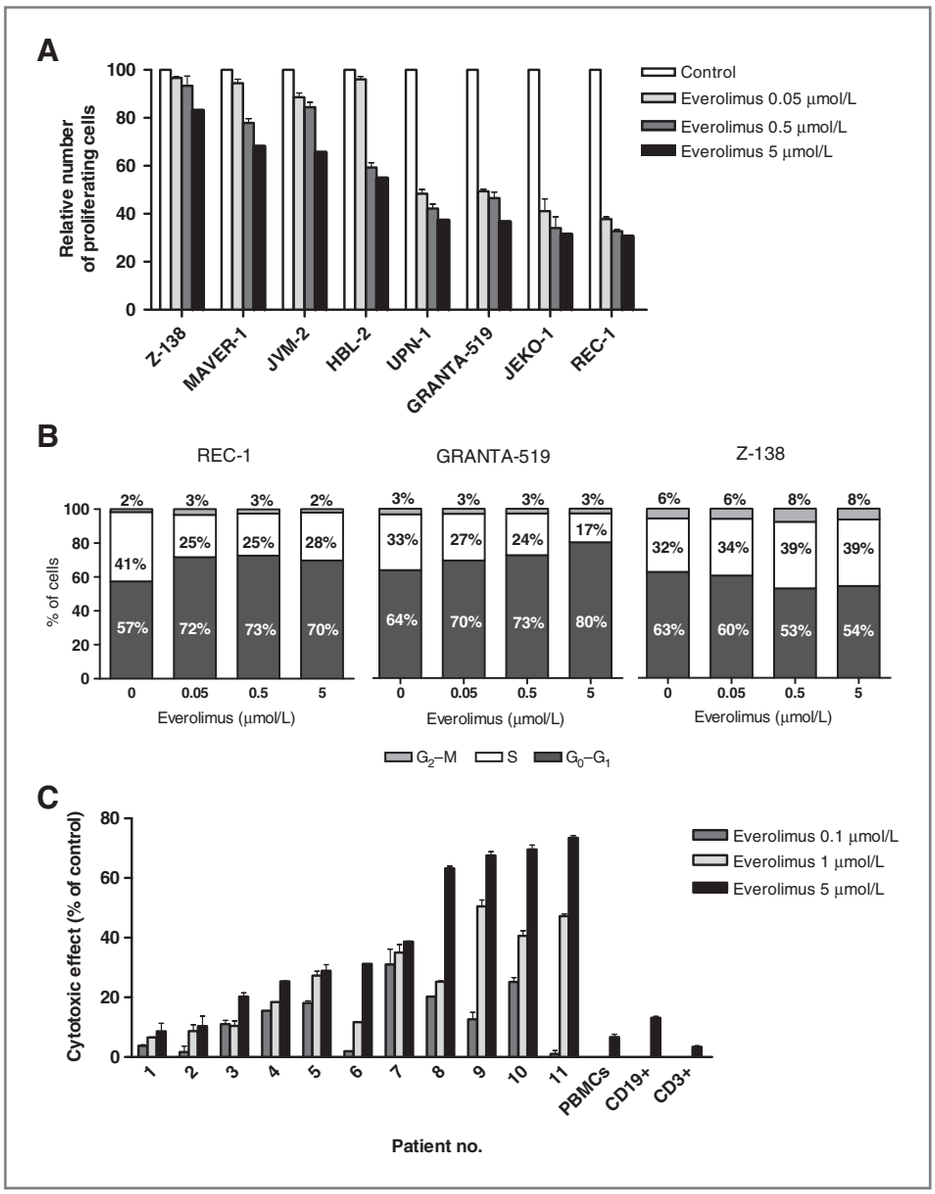

Figure 1. Everolimus antiproliferative effect in mantle cell lymphoma (MCL) cells. A, MCL cell lines were incubated for 72 hours with increasing doses of everolimus (0.05–5 μmol/L) before drug cytostatic effect was analyzed by MTT proliferation assay. B, REC-1, GRANTA-519, and Z-138 cells were treated for 72 hours with everolimus (0.05–5 μmol/L) and cell-cycle fractions were determined by flow cytometry of propidium iodide-labeled nuclei. C, MCL primary cells and peripheral blood mononuclear cells from healthy donors were incubated with everolimus (0.1, 1, and 5 μmol/L) and cytotoxicity was assessed by cytofluorimetric analysis of Annexin V labeling at 48 hours as described in Materials and Methods.

mTOR activity in a representative sensitive MCL primary sample (Fig. 2D), as established by lower levels of phosphorylated mTOR, Akt, S6RP, and 4E-BP1, without observing compensatory reactivation of Akt after 48 hours of incubation.

Altogether, these data indicate that although everolimus inhibits mTOR pathway at short time treatment, Akt rephosphorylation after prolonged exposure could limit its efficacy, consistent with the existence of feedback loops within the mTOR signaling pathway, as described previously (14, 19).

Akt targeting increases everolimus activity in MCL cells

To investigate the impact of the Akt rephosphorylation in MCL cells exposed to everolimus, REC-1, GRANTA-519, and Z-138 cell lines were pretreated with or without 2 or 5 μmol/L of the Akt inhibitor Akti-1/2 for 3 hours and incubated with everolimus at 0.5 and 5 μmol/L for 24 additional hours. As shown on Fig. 3A, MCL cell viability was almost unaffected by Akti-1/2, whereas its addition to everolimus allowed to reduce cell viability more efficiently than single drug treatment. We found the combination of everolimus 5 μmol/L with Akti-1/2 5 μmol/L to be synergistic in REC-1 and GRANTA-519 cells, with respective CI values of 0.691 and 0.602. In contrast, this combination failed to induce cytotoxicity in the everolimus-low sensitive cell line Z-138 (Fig. 3A), although it allowed a synergistic cytostatic effect, as monitored by MTT assay (Supplementary Fig. S1). Of note, the combination of both agents was synergistic in all the MCL primary cells tested ($n = 8$),

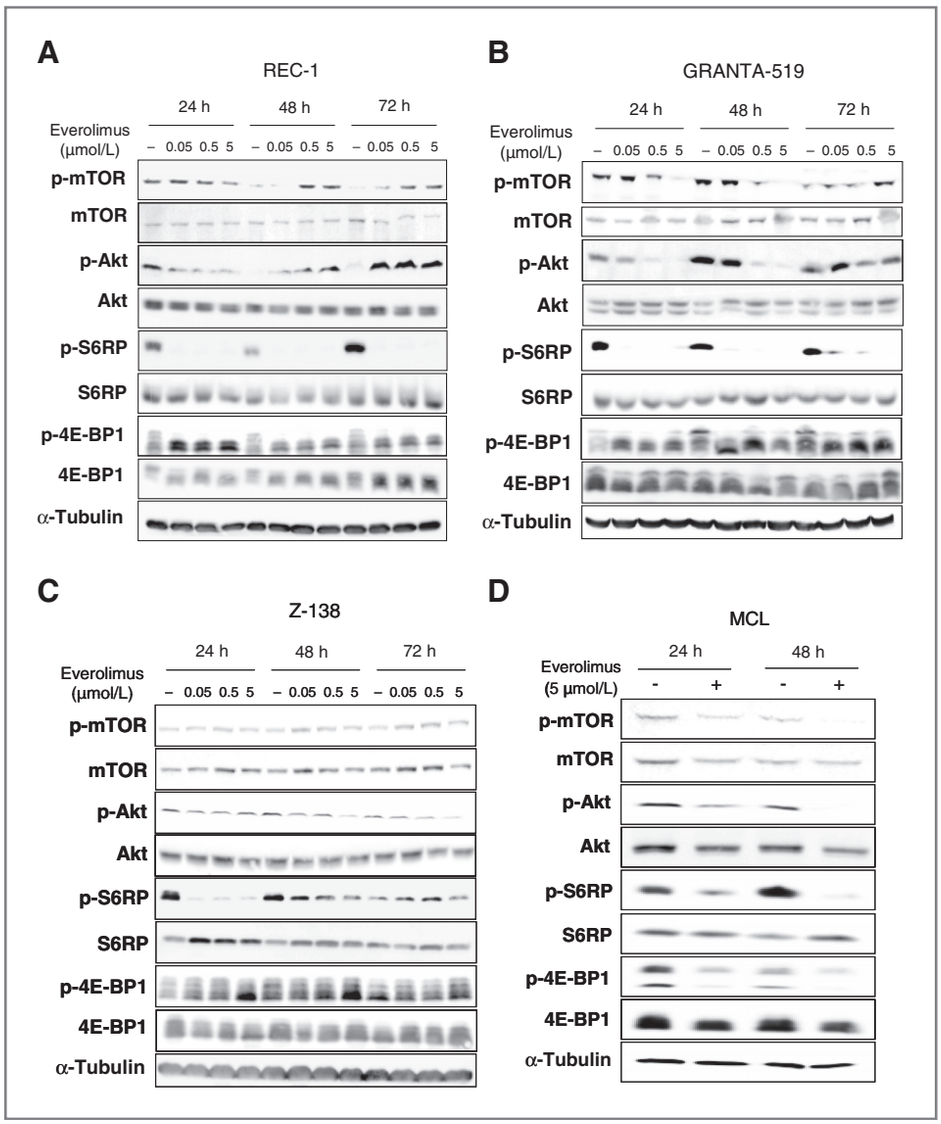

Figure 2. Modulation of mTOR pathway in mantle cell lymphoma (MCL) cells exposed to everolimus. REC-1 (A), GRANTA-519 (B), Z-138 (C), and a representative MCL primary sample (patient no. 11; D) were incubated with everolimus at the indicated doses and times. The levels of phosphorylated and total mTOR pathway proteins (mTOR, Akt, S6RP, and 4E-BP1) were determined by Western blot. The different isoforms of 4E-BP1 represent the phosphorylation status of the protein, with the highest and the lowest bands corresponding to the hyperphosphorylated and the hypophosphorylated forms, respectively. α-tubulin was probed as an equal loading control.

although a significant increase ($P < 0.001$) in cell death induction was only observed in the subset of MCL cases sensitive to everolimus single agent, with a mean CI value of 0.229 (Fig. 3B).

In an attempt to analyze the mechanisms underlying the combinatory effect of Akti-1/2 and everolimus, both REC-1 and Z-138 cells were treated for 24 and 48 hours with everolimus and/or Akti-1/2, followed by Western blot of Akt/mTOR pathway status. Figure 3C shows that Akti-1/2 efficiently blocked Akt phosphorylation in both cell lines, including when added to everolimus. This effect, combined with everolimus inhibitor activity against the mTOR targets p-S6RP and p-4E-BP1, led to the activating processing of the effector caspase-3 and degradation of the caspase substrate PARP in REC-1, but not in Z-138 cells, indicating a defect in apoptosis induction after Akt inhibition in Z-138 cells (Fig. 3C).

These results show a synergistic interaction between everolimus and the Akt inhibitor Akti-1/2 in MCL cells, suggesting a role for Akt signaling in MCL resistance to mTOR targeting.

Everolimus/Akti-1/2 low-responsive MCL cells have increased levels of autophagy

The Akt/mTOR pathway has been implicated in the regulation of autophagy in several models of cancer (20, 21). To explain the heterogeneous efficacy of everolimus/Akti-1/2 combination in MCL cells, we assessed the degree of autophagy induction in Z-138 and REC-1 cells. Western blot analysis of the autophagy-initiating protein LC3B showed that everolimus/Akti-1/2 treatment led to the processing of LC3B-I to LC3B-II, indicative of an increase in the autophagic activity (Fig. 4A). Importantly, this phenomenon was mainly observed in the everolimus/Akti-1/2

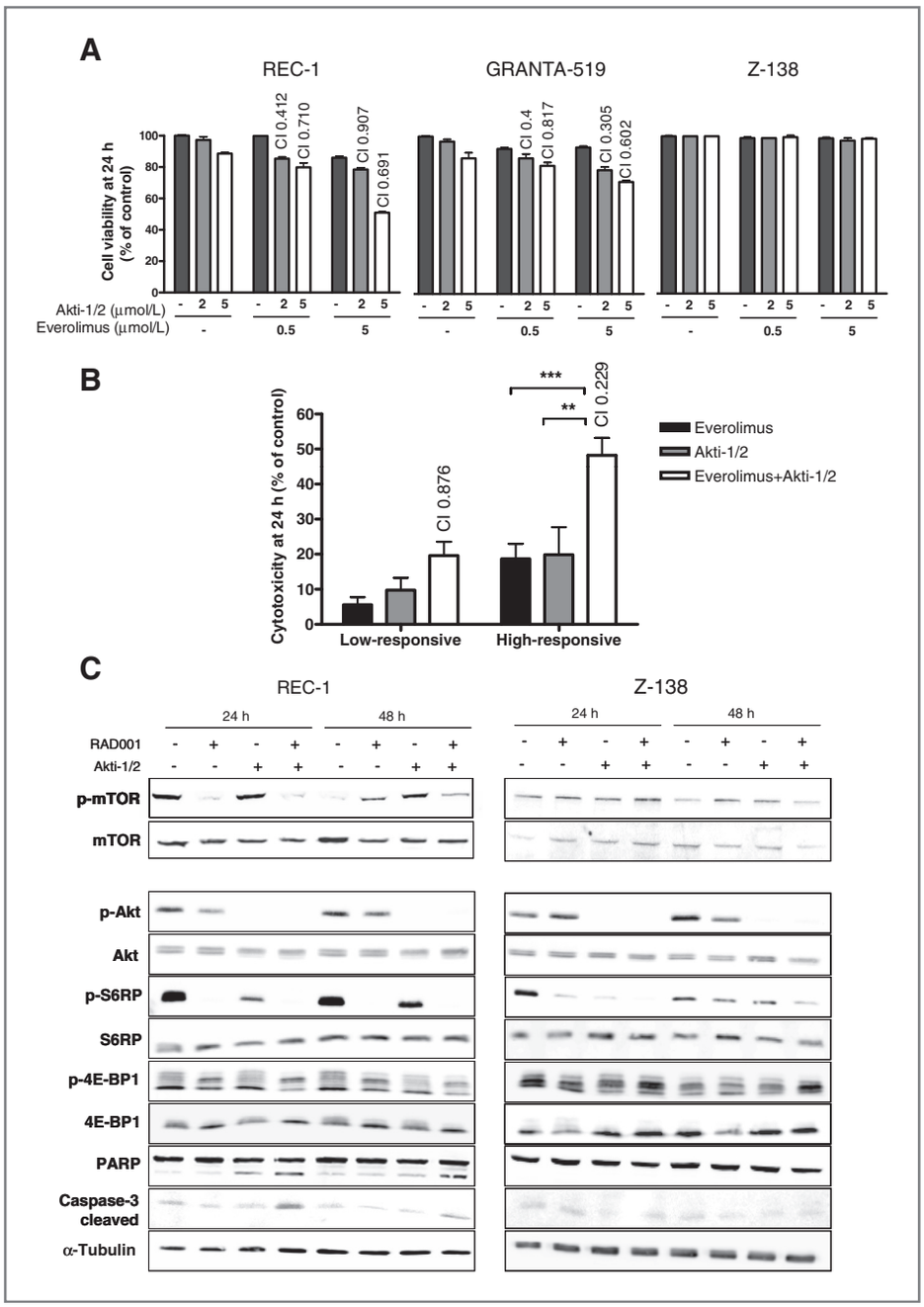

Figure 3. Synergistic effect of everolimus and the Akt inhibitor Akti-1/2. A, REC-1, GRANTA-519, and Z-138 cells were pretreated with Akti-1/2 for 3 hours and incubated with everolimus for 24 hours at the indicated doses. Cell viability was analyzed by flow cytometry labeling of AnnexinV/PI. Combination index (CI) value is indicated for each combination. B, primary MCL cells were pretreated for 3 hours with 5 μmol/L Akti-1/2, followed by an additional 24-hour exposure to 5 μmol/L everolimus. Bars represent the mean ± SEM of cell death referred to untreated control for everolimus low-responsive ($n = 4$) and high-responsive ($n = 4$) cells. Statistical significance was assessed by 2-way ANOVA test (**, $P < 0.01$; ***, $P < 0.001$). CI value is indicated for each combination. C, REC-1 and Z-138 cells were preincubated with 5 μmol/L Akti-1/2 for 3 hours and treated with 5 μmol/L everolimus for 24 or 48 hours before Western blot analysis. α-tubulin was probed as an equal loading control.

low-responsive Z-138 cells (ratio LC3B-II/α-tubulin of 5.8), compared with the sensitive cells REC-1 (ratio LC3B-II/α-tubulin of 2.4). As LC3B-II is known to specifically associate with the autophagosome membrane, we then studied the production of autophagic vacuoles in REC-1 and Z-138 cells. Both cell lines were pretreated with Akti-1/2 (5 μmol/L, 3 hours) and incubated with everolimus. After 24 hours of treatment, cells were stained with the autophagy Cyto-ID Green dye, and then analyzed by flow cytometry. Tamoxifen (22) and bafilomycin A1-treated cells (23, 24) were used as a positive and negative control for autophagolysosome detection, respectively (Fig. 4B). In REC-1 cells, everolimus/Akti-1/2 treatment provoked a slight green fluorescence increase, indicative of some levels of autophagy induction. In contrast, in Z-138 cells, everolimus and Akti-1/2 alone, but especially the combination of both drugs, caused a 5-fold increase in mean fluorescence intensity, revealing an enhanced autophagolysosome formation by dual Akt/mTOR targeting.

To provide further evidence of the autophagy stimulation after everolimus/Akti-1/2 treatment, we studied the accumulation of Cyto-ID Green stained autophagolysosomes

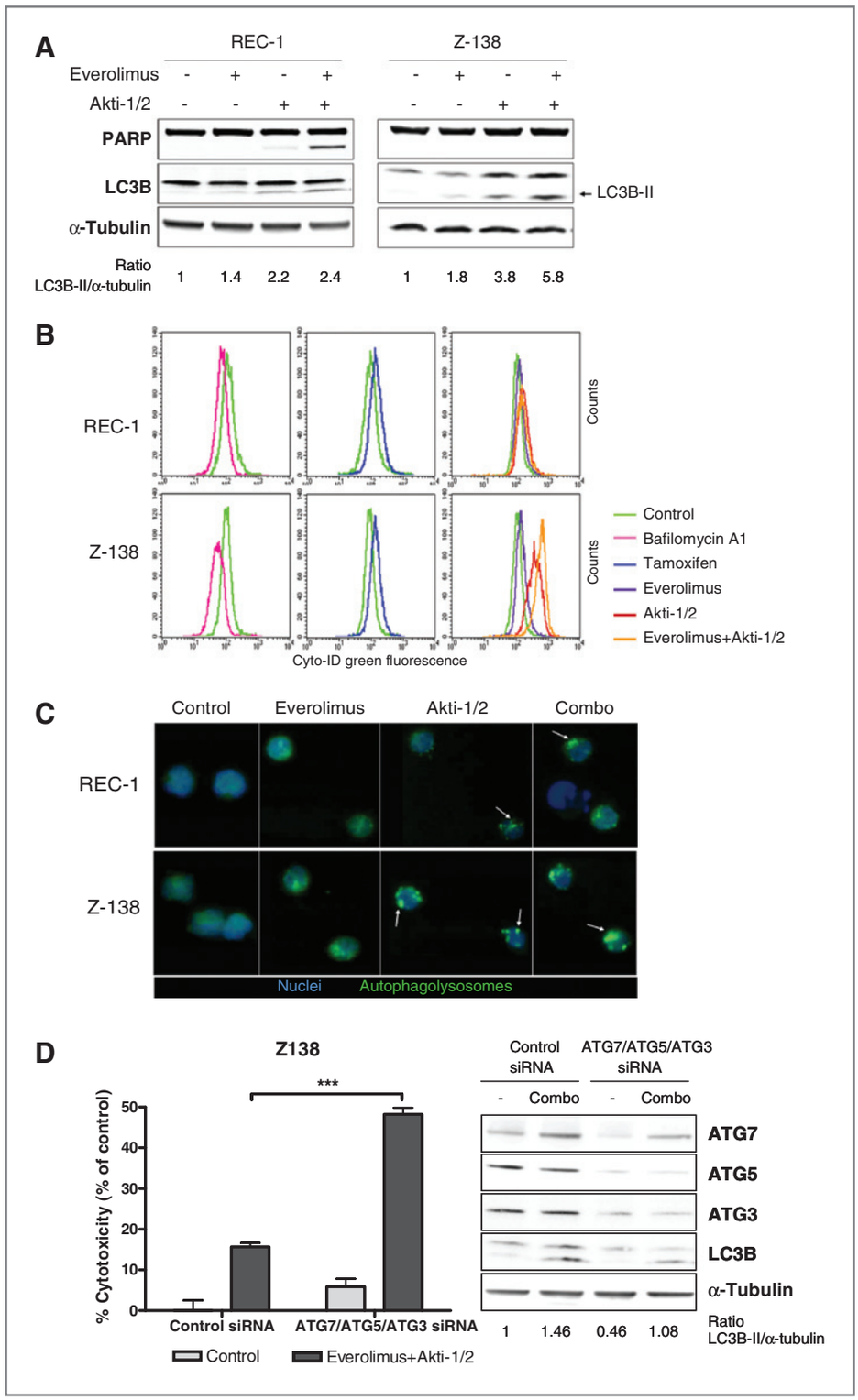

Figure 4. Increased levels of autophagy in everolimus/Akti-1/2 low-responsive cells. A, PARP and LC3B expression were analyzed by Western blot in REC-1 and Z-138 cells after a 3-hour preincubation with 5 μmol/L Akti-1/2, followed by a 24-hour treatment with 5 μmol/L everolimus. α-tubulin was probed as an equal loading control. Ratio between α-tubulin and LC3B-II levels was calculated and relative protein quantification in treated versus control extracts was conducted with Image Gauge software (Fujifilm). B and C, autophagy was determined by detection of Cyto-ID Green stained autophagolysosomes by flow cytometry or fluorescence microscopy in REC-1 and Z-138 cells treated as above with everolimus, Akti-1/2, or both agents (combo). A 24-hour treatment with bafilomycin A1 (5 nmol/L for REC-1 and 50 nmol/L for Z-138 cells) or tamoxifen (24 hours, 10 μmol/L) was used as negative and positive controls of autophagy, respectively. High fluorescence intensity punctuate pattern corresponds to the production of autophagolysosomes (arrows). D, Z-138 cells were transfected by electroporation with *ATG7/ATG5/ATG3* siRNA mix and nonsilencing siRNA. Transfected cells were then preincubated with 5 μmol/L Akti-1/2 for 3 hours previously to everolimus treatment for 20 additional hours. Viability was assessed by flow cytometry labeling of AnnexinV/PI and knockdown of ATG proteins, as well as LC3B processing, were checked by Western blot. α-tubulin was probed as a loading control. LC3B-II/α-tubulin ratio was calculated as previously. Statistical significance was assessed by 2-way ANOVA test (***, $P < 0.001$).

by fluorescence microscopy (Fig. 4C). Untreated control cells harbored a diffuse distribution of green fluorescence throughout the cytoplasm, whereas treated cells presented punctuate structures corresponding to the autophagic vacuoles. As shown in Fig. 4C, we observed a substantial autophagy induction after Akti-1/2 treatment in both REC-1 and Z-138 cells (arrows), but the addition of everolimus notably increased the autophagic flux (arrows). Consistently,

this effect was more pronounced in the everolimus/Akti-1/2 low-responsive Z-138 cells than in the sensitive cells REC-1.

To ascertain if this increase in autophagy could promote MCL cell survival and drug resistance, we used a siRNA-mediated approach to simultaneously knockdown the ubiquitin-like activating enzyme homolog ATG7, the ubiquitin folds-containing protein ATG5, and the ubiquitin-conjugating enzyme analog ATG3, all involved in LC3 activation. *ATG7*/*ATG5*/*ATG3* triple silencing reduced the basal protein levels of these 3 factors, thereby decreasing LC3B-II expression and significantly enhancing cell death after everolimus/Akti-1/2 treatment in Z-138 cell line ($P < 0.001$, Fig. 4D). A sensitizing effect, albeit reduced, was also observed in REC-1 cells (data not shown), emphasizing the role of autophagy in Z-138 resistance to everolimus/Akti-1/2 combination.

These findings highlight the contribution of autophagy to the resistance to everolimus/Akti-1/2 treatment in MCL cells.

Inhibition of autophagic vacuoles sensitizes MCL cells to everolimus/Akti-induced apoptosis

In an attempt to counteract the protective effect of autophagy toward everolimus/Akti-1/2 treatment, we assessed the effect of adding an autophagy inhibitor to increase the antitumoral effect of the combination. We used hydroxychloroquine, an antimalarial drug that blocks lysosome acidification and degradation of autophagosomes, causing an accumulation of autophagic vacuoles (25). REC-1 and Z-138 cells were preincubated with hydroxychloroquine 10 μmol/L for 1 hour, then pretreated with 5 μmol/L Akti-1/2 for 3 hours and finally incubated with 5 μmol/L everolimus for 24 hours. Although this triple combination led to a significant induction of apoptosis in both MCL cell lines, this effect was highly significant ($P < 0.001$) in the everolimus/Akti-1/2 low sensitive Z-138 cells (Fig. 5A). As expected, hydroxychloroquine addition to the everolimus/Akti-1/2 treatment provoked an increase of LC3B-II expression in both cell lines (Fig. 5B). Moreover, the triple combination increased PARP cleavage in REC-1 cells and also in Z-138 cells, where the everolimus/Akti-1/2 treatment did not exert any cytotoxic effect (Fig. 5B). Similar results were obtained with bafilomycin A1, another autophagy inhibitor (data not shown).

We then tested the effect of combining hydroxychloroquine with the Akt/mTOR inhibitors in MCL primary cases. Although hydroxychloroquine addition synergized with Akti-1/2 and everolimus in all MCL cases tested, only those cases with poor response to the everolimus/Akti-1/2 combination had a significant increase in cell death ($P < 0.01$; Fig. 5C).

Accordingly, while combination of everolimus and Akti-1/2 slightly activated the mitochondrial apoptotic pathway in low responsive MCL cells (Z-138 and a representative MCL primary sample), the addition of hydroxychloroquine enhanced the typical mitochondrial hallmarks of apoptosis, including mitochondrial depolarization, ROS production, caspase-3/7 activity, and PS exposure (Fig. 5D).

Taken together, these results show that the addition of an autophagy inhibitor overcomes the resistance of MCL cells to Akt/mTOR inhibitors, leading to efficient apoptosis induction and suggesting a prosurvival role of autophagy.

Discussion

The PI3K/Akt/mTOR axis is known to be constitutively activated in the majority of B-cell lymphomas. In these cancers, mTOR-activating events may include loss of PTEN function, leading to constitutive activation of Akt, constitutional or growth factor–induced stimulation of receptor tyrosine kinases, or overexpression of eIF4E (26). Specifically, in the blastoid variant of MCL, high levels of phosphorylation on Akt at Ser473 are frequently observed (27).

To target this pathway, several rapamycin analogs have shown activity against lymphoma cells both *in vitro* and *in vivo* (28). Here, using an extended panel of MCL cell lines, we confirm previous reports showing that the rapalog everolimus exerts an antiproliferative effect in MCL cell lines, mediated by cell-cycle blockade at G_1 phase (29). We also show for the first time that this agent induces a tumor-selective, dose-dependent cytotoxicity in the majority of primary MCL cases, in the range of doses achievable *in vivo*. As expected, we show that everolimus efficiently inhibits mTOR activity in sensitive cell lines and primary samples, as attested by a decrease in the phosphorylation levels of the mTOR downstream targets S6RP and 4E-BP1 at short-time treatment, and a transient dephosphorylation of Akt at Ser473. Importantly, we observe that prolonged mTORC1 inactivation leads to Akt rephosphorylation at this residue, a phenomenon described as a crucial determinant of malignant cell response to rapamycin-like drugs (14, 19). Suggesting that this late reactivation of Akt may counteract everolimus activity, we report that the combination of the rapalog to an isoselective Akt inhibitor exerts synergistic antitumoral activity in all the samples tested, especially in those cases with high sensitivity to everolimus single agent. In these cells, we show the effect of the combination to be mediated by activation of the intrinsic apoptotic program, whereas everolimus alone appears to be a weak apoptosis inducer, as previously reported for rapamycin (30).

Several evidences suggest that the synergism between Akt and mTOR dual targeting may rely on the blockade of the mTORC1-dependent response loop after mTOR inhibition, which has been shown to involve reactivation of upstream receptor kinase signaling within the IGFR pathway, as well as Akt itself, in both *in vitro* and *in vivo* models of human cancers (5, 31, 32). Emerging from this observation, the use of dual PI3K/mTOR inhibitors has shown to be useful not only to downregulate the mTOR targets 4E-BP1 or S6RP, but also to prevent Akt rephosphorylation at Ser473, independent of PI3K mutation status (33). In line with our results, the complete abolition of Akt/mTOR signaling by means of these dual inhibitors has been shown to exert increased cytostatic effect and to lead to apoptotic cell death in PI3K/Akt/mTOR-addicted lymphomas (34, 35), thus highlighting the requirement of a full inhibition of the pathway for

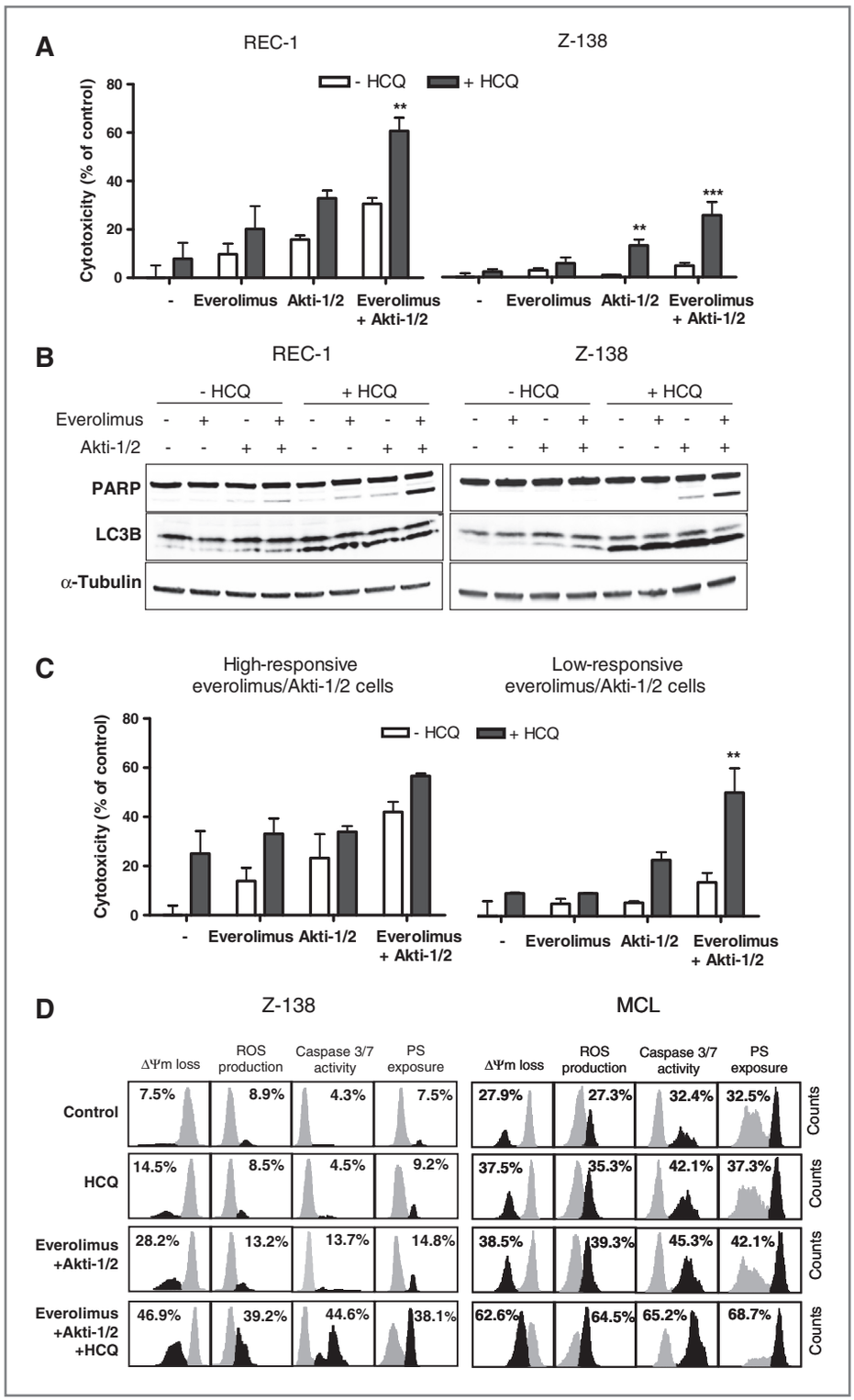

Figure 5. The autophagy inhibitor hydroxychloroquine overcomes the resistance to everolimus/Akti-1/2 inhibitors. A, REC-1 and Z-138 cells were pretreated with 50 μmol/L hydroxychloroquine (HCQ) for 1 hour, followed by 3-hour incubation with 5 μmol/L Akti-1/2 and exposure to 5 μmol/L everolimus for 24 hours. Cytotoxicity was determined by flow cytometry labeling of AnnexinV/PI. Bars represent the mean ± SEM of cell death referred to control cells. Statistical significance was assessed by 2-way ANOVA test (**, $P < 0.01$; ***, $P < 0.001$). B, REC-1 and Z-138 cells were treated as above for 24 hours. PARP and LC3B expression was analyzed by Western blot. α-tubulin was probed as an equal loading control. C, primary MCL samples from the high-responsive ($n = 3$) and the low-responsive ($n = 3$) everolimus/Akti-1/2 group were preincubated with 10 μmol/L HCQ for 1 hour before treatment with 5 μmol/L Akti-1/2 for 3 hours and an additional 24-hour exposure to 5 μmol/L everolimus. Statistical significance was assessed by 2-way ANOVA test (**, $P < 0.01$; $n = 3$). D, Z-138 cells and a representative everolimus/Akti-1/2 low-responsive MCL sample were treated with HCQ (50 μmol/L for Z-138, 10 μmol/L for MCL primary cells), Akti-1/2, and everolimus as above for 48 hours and typical apoptosis hallmarks were determined by flow cytometry as described in Materials and Methods. Percentages inside each chart refer to the population in black.

improved antitumoral activity. However, we observed that those MCL samples that are weak responders to everolimus single agent still harbor a high viability rate despite the complete Akt/mTOR axis inhibition, similar to a previous observation in follicular lymphoma (35). Among the resistance mechanisms that may account for this defective apoptosis initiation, accumulating evidences suggest that autophagy is one of the major process functionally involved

in cancer cell survival after Akt and mTOR inhibitor exposure (36).

Autophagy is an evolutionarily conserved intracellular self-defense mechanism, which serves to maintain cellular metabolism through recycling of cellular components when the availability of external nutrient sources is limited (36). Although constitutive autophagy is a homeostatic mechanism for metabolic regulation, it is also stress responsive, and through the removal of damaged proteins and organelles, it confers stress tolerance and sustains viability under adverse conditions (37). mTOR kinase inhibition has been shown to induce a prosurvival autophagy that can counteract the effect of common chemotherapeutics in colon carcinoma (38). In MCL cells, the rapalog temsirolimus has also been shown to activate autophagic processing, although the contribution of this phenomenon to the activity of the mTOR inhibitor was not clearly discussed (39). Our results show that 2 hallmarks of autophagy, LC3B processing and autophagic vacuoles formation, are enhanced in MCL cells resistant to everolimus/Akti-1/2 combination, when compared with sensitive cells. More important, we show that autophagy controls MCL response to mTOR/Akt inhibitors, as knockdown of ATG7, ATG5, and ATG3, all 3 proteins required for the progression of autophagy, allows MCL cells to undergo apoptosis upon exposure to the combination. Accordingly, it has been described that dual inhibitors of PI3K/mTOR kinases may induce autophagy as a central survival signal (40), pointing out that effective cell death in malignant cells with constitutive Akt activation would require the blockade of the 3 targets we describe herein: mTOR, Akt, and autophagy.

As autophagy is generally a survival pathway used by tumor cells to tolerate metabolic stress (22, 41), autophagy inhibitors, in combination with other agents, are expected to efficiently target therapy-resistant tumor cells in hypoxic tumor regions (37). Compounds such as hydroxychloroquine or chloroquine that block lysosome acidification and consequent autophagosome fusion, have been entered in a number of clinical trials in combination with standard or experimental agents (42). In hematologic malignancies, these agents are being tested in combination with the proteasome inhibitor bortezomib in multiple myeloma (NCT00568880; ref. 36) or with the histone deacetylase inhibitor vorinostat in chronic myeloid leukemia (43). These latest studies sustain the concept that autophagy is a mechanism of therapeutic resistance, and that hydroxychloroquine can increase cytoxicity by abrogation of autophagy. In accordance with this, we found that the addition of this agent to everolimus/Akti-1/2 combination fully activates the intrinsic apoptotic program in MCL cells primarily resistant to Akt/mTOR dual targeting.

In summary, we show for the first time that the use of an autophagy inhibitor may overcome resistance to the combination of everolimus and an isoselective Akt inhibitor in MCL cell lines and primary samples. The proposed prosurvival role of autophagy in Akt/mTOR compromised cells points out some potential opportunities and warrant further clinical activity of this triple combinational strategy in MCL patients.

Disclosure of Potential Conflicts of Interest

No potential conflicts of interest were disclosed.

Authors' Contributions

Conception and design: L. Rosich, D. Colomer, G. Roué
Development of methodology: L. Rosich, M. Lopez-Guerra, D. Colomer, G. Roué
Acquisition of data (provided animals, acquired and managed patients, provided facilities, etc.): L. Rosich, D. Colomer, G. Roué
Analysis and interpretation of data (e.g., statistical analysis, biostatistics, computational analysis): L. Rosich, S. Xargay-Torrent, E. Campo, D. Colomer, G. Roué
Writing, review, and/or revision of the manuscript: L. Rosich, M. Lopez-Guerra, E. Campo, D. Colomer, G. Roué
Study supervision: D. Colomer, G. Roué
Revision of the final version of the manuscript: S. Xargay-Torrent, G. Roué

Acknowledgments

The authors thank Jocabed Roldán, Laura Jiménez, and Sandra Cabezas for expert technical assistance and Anna Bellmunt for her help in *in vitro* studies. Everolimus was kindly provided by Novartis. This work was carried out, in part, at the Esther Koplowitz Center, Barcelona.

Grant Support

Fondo de Investigación Sanitaria (PI09/0060; to G. Roué), Ministerio de Ciencia e Innovación (SAF 09/9503; to D. Colomer), Redes Temáticas de Investigación Cooperativa de Cáncer from the Instituto de Salud Carlos III (RED 2006-20-014 to D. Colomer and 2006-20-039 to E. Campo), and Generalitat de Catalunya (2009SGR967 to D. Colomer). L. Rosich and S. Xargay-Torrent are recipients of predoctoral fellowships from IDIBAPS and Ministerio Ciencia e Innovación (FPU), respectively. M. López-Guerra has a contract from RED 2006-20-014.

The costs of publication of this article were defrayed in part by the payment of page charges. This article must therefore be hereby marked *advertisement* in accordance with 18 U.S.C. Section 1734 solely to indicate this fact.

Received February 1, 2012; revised July 12, 2012; accepted August 2, 2012; published OnlineFirst August 9, 2012.

References

1. Jares P, Colomer D, Campo E. Genetic and molecular pathogenesis of mantle cell lymphoma: perspectives for new targeted therapeutics. Nat Rev Cancer 2007;7:750–62.
2. Perez-Galan P, Dreyling M, Wiestner A. Mantle cell lymphoma: biology, pathogenesis, and the molecular basis of treatment in the genomic era. Blood 2011;117:26–38.
3. Drakos E, Rassidakis GZ, Medeiros LJ. Mammalian target of rapamycin (mTOR) pathway signalling in lymphomas. Expert Rev Mol Med 2008;10:e4.
4. Guertin DA, Sabatini DM. Defining the role of mTOR in cancer. Cancer Cell 2007;12:9–22.
5. Sparks CA, Guertin DA. Targeting mTOR: prospects for mTOR complex 2 inhibitors in cancer therapy. Oncogene 2010;29:3733–44.
6. Faivre S, Kroemer G, Raymond E. Current development of mTOR inhibitors as anticancer agents. Nat Rev Drug Discov 2006;5:671–88.
7. Weniger MA, Wiestner A. Molecular targeted approaches in mantle cell lymphoma. Semin Hematol 2011;48:214–26.
8. Dancey J. mTOR signaling and drug development in cancer. Nat Rev Clin Oncol 2010;7:209–19.
9. O'Donnell A, Faivre S, Burris HA III, Rea D, Papadimitrakopoulou V, Shand N, et al. Phase I pharmacokinetic and pharmacodynamic study

of the oral mammalian target of rapamycin inhibitor everolimus in patients with advanced solid tumors. J Clin Oncol 2008;26:1588–95.
10. Witzig TE, Reeder CB, LaPlant BR, Gupta M, Johnston PB, Micallef IN, et al. A phase II trial of the oral mTOR inhibitor everolimus in relapsed aggressive lymphoma. Leukemia 2011;25:341–7.
11. Ansell SM, Inwards DJ, Rowland KM Jr, Flynn PJ, Morton RF, Moore DF Jr, et al. Low-dose, single-agent temsirolimus for relapsed mantle cell lymphoma: a phase 2 trial in the North Central Cancer Treatment Group. Cancer 2008;113:508–14.
12. Witzig TE, Geyer SM, Ghobrial I, Inwards DJ, Fonseca R, Kurtin P, et al. Phase II trial of single-agent temsirolimus (CCI-779) for relapsed mantle cell lymphoma. J Clin Oncol 2005;23:5347–56.
13. Hess G, Herbrecht R, Romaguera J, Verhoef G, Crump M, Gisselbrecht C, et al. Phase III study to evaluate temsirolimus compared with investigator's choice therapy for the treatment of relapsed or refractory mantle cell lymphoma. J Clin Oncol 2009;27:3822–9.
14. Meric-Bernstam F, Akcakanat A, Chen H, Do KA, Sangai T, Adkins F, et al. PIK3CA/PTEN mutations and Akt activation as markers of sensitivity to allosteric mTOR inhibitors. Clin Cancer Res 2012;18:1777–89.
15. Lopiccolo J, Blumenthal GM, Bernstein WB, Dennis PA. Targeting the PI3K/Akt/mTOR pathway: effective combinations and clinical considerations. Drug Resist Updat 2008;11:32–50.
16. Swerdlow SH, Campo E, Harris NL, Jaffe ES, Pileri SA, Stein S, et al. WHO classification of tumours of haematopoietic and lymphoid tissues. (4th ed. Lyon, France: International Agency for Research on Cancer ed.; 2008.
17. Bellosillo B, Villamor N, Lopez-Guillermo A, Marce S, Bosch F, Campo E, et al. Spontaneous and drug-induced apoptosis is mediated by conformational changes of Bax and Bak in B-cell chronic lymphocytic leukemia. Blood 2002;100:1810–6.
18. Lee JS, Lee GM. Monitoring of autophagy in Chinese hamster ovary cells using flow cytometry. Methods 2012;56:375–82.
19. O'Reilly KE, Rojo F, She QB, Solit D, Mills GB, Smith D, et al. mTOR inhibition induces upstream receptor tyrosine kinase signaling and activates Akt. Cancer Res 2006;66:1500–8.
20. Degtyarev M, De MA, Klumperman J, Lin K. Autophagy, an Achilles' heel AKTing against cancer? Autophagy 2009;5:415–8.
21. Mathew R, Karantza-Wadsworth V, White E. Role of autophagy in cancer. Nat Rev Cancer 2007;7:961–7.
22. Amaravadi RK, Yu D, Lum JJ, Bui T, Christophorou MA, Evan GI, et al. Autophagy inhibition enhances therapy-induced apoptosis in a Myc-induced model of lymphoma. J Clin Invest 2007;117:326–36.
23. Mizushima N, Yoshimori T, Levine B. Methods in mammalian autophagy research. Cell 2010;140:313–26.
24. Yamamoto A, Tagawa Y, Yoshimori T, Moriyama Y, Masaki R, Tashiro Y. Bafilomycin A1 prevents maturation of autophagic vacuoles by inhibiting fusion between autophagosomes and lysosomes in rat hepatoma cell line, H-4-II-E cells. Cell Struct Funct 1998;23:33–42.
25. Janku F, McConkey DJ, Hong DS, Kurzrock R. Autophagy as a target for anticancer therapy. Nat Rev Clin Oncol 2011;8:528–39.
26. Costa LJ. Aspects of mTOR biology and the use of mTOR inhibitors in non-Hodgkin's lymphoma. Cancer Treat Rev 2007;33:78–84.
27. Rudelius M, Pittaluga S, Nishizuka S, Pham TH, Fend F, Jaffe ES, et al. Constitutive activation of Akt contributes to the pathogenesis and survival of mantle cell lymphoma. Blood 2006;108:1668–76.
28. Coiffier B, Ribrag V. Exploring mammalian target of rapamycin (mTOR) inhibition for treatment of mantle cell lymphoma and other hematologic malignancies. Leuk Lymphoma 2009;50:1916–30.
29. Haritunians T, Mori A, O'Kelly J, Luong QT, Giles FJ, Koeffler HP. Antiproliferative activity of RAD001 (everolimus) as a single agent and combined with other agents in mantle cell lymphoma. Leukemia 2007;21:333–9.
30. Dal CJ, Zancai P, Terrin L, Guidoboni M, Ponzoni M, Pavan A, et al. Distinct functional significance of Akt and mTOR constitutive activation in mantle cell lymphoma. Blood 2008;111:5142–51.
31. Gupta M, Hendrickson AE, Yun SS, Han JJ, Schneider PA, Koh BD, et al. Dual mTORC1/mTORC2 inhibition diminishes Akt activation and induces Puma-dependent apoptosis in lymphoid malignancies. Blood 2012;119:476–87.
32. Sun SY, Rosenberg LM, Wang X, Zhou Z, Yue P, Fu H, et al. Activation of Akt and eIF4E survival pathways by rapamycin-mediated mammalian target of rapamycin inhibition. Cancer Res 2005;65:7052–8.
33. Serra V, Markman B, Scaltriti M, Eichhorn PJ, Valero V, Guzman M, et al. NVP-BEZ235, a dual PI3K/mTOR inhibitor, prevents PI3K signaling and inhibits the growth of cancer cells with activating PI3K mutations. Cancer Res 2008;68:8022–30.
34. Bhatt AP, Bhende PM, Sin SH, Roy D, Dittmer DP, Damania B. Dual inhibition of PI3K and mTOR inhibits autocrine and paracrine proliferative loops in PI3K/Akt/mTOR-addicted lymphomas. Blood 2010;115:4455–63.
35. Bhende PM, Park SI, Lim MS, Dittmer DP, Damania B. The dual PI3K/mTOR inhibitor, NVP-BEZ235, is efficacious against follicular lymphoma. Leukemia 2010;24:1781–4.
36. Amaravadi RK, Lippincott-Schwartz J, Yin XM, Weiss WA, Takebe N, Timmer W, et al. Principles and current strategies for targeting autophagy for cancer treatment. Clin Cancer Res 2011;17:654–66.
37. White E, DiPaola RS. The double-edged sword of autophagy modulation in cancer. Clin Cancer Res 2009;15:5308–16.
38. Huang S, Yang ZJ, Yu C, Sinicrope FA. Inhibition of mTOR kinase by AZD8055 can antagonize chemotherapy-induced cell death through autophagy induction and down-regulation of p62/sequestosome 1. J Biol Chem 2011;286:40002–12.
39. Yazbeck VY, Buglio D, Georgakis GV, Li Y, Iwado E, Romaguera JE, et al. Temsirolimus downregulates p21 without altering cyclin D1 expression and induces autophagy and synergizes with vorinostat in mantle cell lymphoma. Exp Hematol 2008;36:443–50.
40. Fan QW, Cheng C, Hackett C, Feldman M, Houseman BT, Nicolaides T, et al. Akt and autophagy cooperate to promote survival of drug-resistant glioma. Sci Signal 2010;3:ra81.
41. Kovacs JR, Li C, Yang Q, Li G, Garcia IG, Ju S, et al. Autophagy promotes T-cell survival through degradation of proteins of the cell death machinery. Cell Death Differ 2012;19:144–52.
42. Solomon VR, Lee H. Chloroquine and its analogs: a new promise of an old drug for effective and safe cancer therapies. Eur J Pharmacol 2009;625:220–33.
43. Carew JS, Nawrocki ST, Kahue CN, Zhang H, Yang C, Chung L, et al. Targeting autophagy augments the anticancer activity of the histone deacetylase inhibitor SAHA to overcome Bcr-Abl-mediated drug resistance. Blood 2007;110:313–22.